Soft Matter

Formation of Lipid Vesicles in situ Utilizing the Thiol-Michael Reaction

Journal:	*Soft Matter*
Manuscript ID	SM-ART-06-2018-001329.R1
Article Type:	Paper
Date Submitted by the Author:	24-Aug-2018
Complete List of Authors:	Konetski, Danielle; University of Colorado, Department of Chemical and Biological Engineering Baranek, Austin; University of Colorado, Department of Chemical and Biological Engineering Mavila, Sudheendran; University of Colorado, Department of Chemical & Biological Engineering Zhang, Xinpeng; University of Colorado Bowman, Christopher; University of Colorado, Department of Chemical and Biological Engineering

Formation of Lipid Vesicles *in situ* Utilizing the Thiol-Michael Reaction

Danielle Konetski[a], Austin Baranek[a], Sudheendran Mavila[a], Xinpeng Zhang[a] and Christopher N. Bowman[a]*

a. *Department of Chemical and Biological Engineering, University of Colorado, 3415 Colorado Avenue, JSC Biotech Building, Boulder, Colorado 80303, United States*

*christopher.bowman@colorado.edu *(303-492-3247)*

Abstract

Synthetic unilamellar liposomes, functionalized to enable novel characteristics and behavior, are of great utility to fields such as drug delivery and artificial cell membranes. However, the generation of these liposomes is frequently highly labor-intensive and time consuming whereas *in situ* liposome formation presents a potential solution to this problem. A novel method for *in situ* lipid formation is developed here through the covalent addition of a thiol-functionalized lysolipid to an acrylate-functionalized tail *via* the thiol-Michael addition reaction with potential for inclusion of additional functionality via the tail. Dilute, stoichiometric mixtures of a thiol lysolipid and an acrylate tail reacted in an aqueous media at ambient conditions for 48 hours reached nearly 90% conversion, forming the desired thioether-containing phospholipid product. These lipids assemble into a high density of liposomes with sizes ranging from 20nm to several microns in

diameter and include various structures ranging from spheres to tubular vesicles with structure and lamellarity dependent upon the catalyst concentration used. To demonstrate lipid functionalization, an acrylate tail possessing a terminal alkyne was coupled into the lipid structure. These functionalized liposomes enable photo-induced polymerization of the terminal alkyne upon irradiation.

Introduction

In the fields of drug[1–5] and cosmetics delivery[6–8], cellular membrane modeling[9–13], artificial cell design[14–21], microreactor development[22–25] as well as others, phospholipid-based vesicles have found great potential since their discovery in the early 1960s[26]. Composed primarily of phospholipid molecules, these lipid vesicles, or liposomes, mimic cell membranes. Lipids are assembled with charged head-groups extended into solution and hydrophobic tail domains sequestered into the middle of the bilayer. The bilayers enwrap an internal aqueous compartment, effectively separating it from the surrounding media, minimizing contact of the hydrophobic chains with the aqueous environment. This lipid-water interface enables encapsulation of hydrophobic molecules within the bilayer and hydrophilic compounds inside the interior compartment, thereby imparting their utility on this wide range of fields.

However, while their structure is ideal for encapsulation, to enable the use of liposomes for many of these applications, it becomes necessary to introduce novel behavior, responsiveness or other characteristics into the phospholipid membrane[27]. For example, synthetic phospholipid molecules bearing functionalities[27] such as photo-cleavable structures[28], double or triple bonds for polymerization [29,30], isomerizable structures[31] and porphyrin rings[32,33] have been studied to induce permeability of the membrane for stimuli-responsive drug delivery. However, in order to generate and utilize these lipids, intensive and complicated syntheses are often necessary, resulting in a more laborious and time-consuming design-build-test process.

Recently, a new method for the *in situ* formation of phospholipid molecules was developed for covalently attaching a hydrophobic tail to a functionalized lysolipid backbone utilizing the copper-catalyzed azide-alkyne cycloaddition (CuAAC) reaction[34–36]. This lipid formation method could be employed to enable simplified incorporation of synthetic moieties into the lipid structure to generate designer lipids. However, many systems are not amenable to the copper catalyst necessary for the CuAAC reaction due to ligand-dependent toxicity effects in living systems[37–39]. Alternatively, the functionality of interest may not be orthogonal to the redox reaction necessary to generate the Cu(I) catalyst or if a terminal alkyne functionality is to be incorporated in the tail this formation chemistry could not be used. More recently, imine, native chemical ligation and thioester exchange chemistries have been utilized to form synthetic liposomes capable of continued exchange[40–42]; however, this instability could be detrimental to the implementation of liposomes for commercial applications. In contrast, the thiol-Michael click reaction has enhanced biocompatibility in that it avoids the use of Cu, is readily catalyzed by relatively weak bases and nucleophiles, is amenable to the aqueous conditions required for *in situ* liposome formation, proceeds rapidly to completion under ambient conditions without significant side reactions, and is compatible with the usage of a wide range of natural and synthetic thiols as well as alkene functionalities. In this reaction, thiol groups and electron deficient alkenes such as acrylates, maleimides, vinyl sulfones and others undergo coupling in the presence of basic or nucleophilic catalysts *via* a thiolate anion intermediate to produce a thioether product[43]. To increase the range of designer lipid systems compatible

with the *in situ* formation method, we have incorporated acrylate and thiol functionalities into the tail and lysolipid structures, respectively, to enable thiol-Michael formation of phospholipids. The power of this formation chemistry lies in the fact that this system is not limited to the acrylate tail used here. By utilizing the thiol-Michael addition reaction, lipids are functionalized using any number of acrylate and methacrylate monomers available for commercial purchase, and new vinyl sulfone or acrylate monomers can be easily synthesized from compounds of interest bearing free hydroxyl groups. Additionally, vast quantities of bioconjugate chemistry have revolved around the use of maleimide-functionalized molecules and cysteine-functionalized peptides, making each of those systems immediately available for use as the ene or thiol, respectively, in this synthetic membrane formation method. Beyond the array of molecules available for use in the thiol-Michael reaction, the use of photo-bases[44,45] for photo-initiated thiol-Michael reactions enables spatiotemporal control in liposome formation using this method.

Results and Discussion

Expanding the reaction toolbox for the generation of synthetic phospholipids

The highly efficient thiol-Michael addition reaction was employed to form a functionalized phospholipid (see 3 in Scheme 1) *via* functionalization of the lysolipid with a primary thiol [1] and the subsequent nucleophile-catalyzed reaction of the thiol with an aliphatic acrylate tail [2] as shown in Scheme 1. This approach enables the design and implementation of an incredible range of new, functionalized phospholipids based on aliphatic tails, other functionalized molecules chosen from

the great variety of acrylate monomers already commercially available, molecules that are readily formed by reactions of acids or other terminal functional groups, or the array of maleimide-functionalized bioconjugate molecules available.

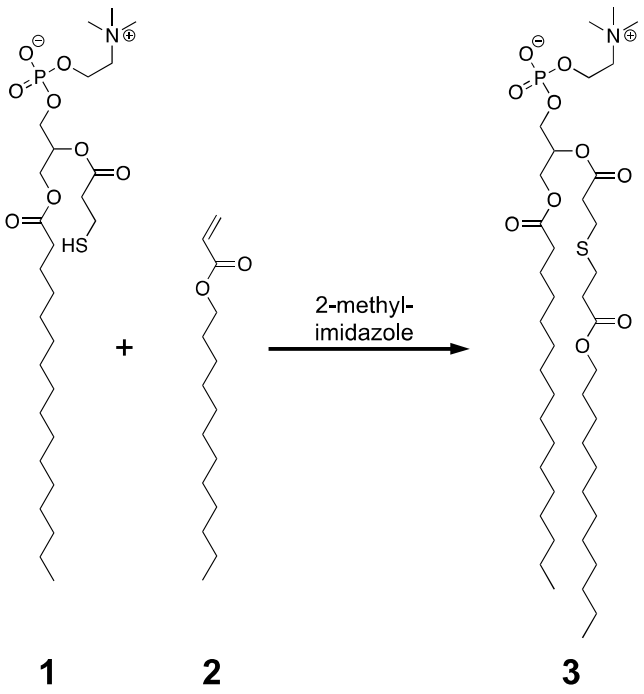

Scheme 1. A lysolipid bearing a free thiol functionality (1) readily and rapidly undergoes thiol-Michael addition with an acrylate functionalized tail (2) in the presence of a water-soluble, nucleophile catalyst, 2-methylimidazole, to produce a thioether-containing phospholipid product (3). The precursors in this process assemble into micelles and stabilized oil droplets and transition to bilayer structures and liposomes *in situ* upon addition of the second aliphatic tail and the subsequent Michael addition reaction.

SHPC and the aliphatic acrylate tail (AT) were mixed at a concentration of 5mM in the presence of 2.5mM of a water-soluble nucleophile catalyst, 2-methylimidazole. A weak base catalyst, triethylamine (TEA), was also explored as a

potential catalyst. However, at the dilute conditions necessary, the reaction rates were exceedingly slow whereas increased concentrations of TEA leads to hydrolytic degradation of the esters present in the lipid structures. Stronger nucleophiles were probed as well, but suffered from limitations in aqueous solubility. Samples drawn at various time points were injected into an analytical LC-MS equipped with an Evaporative Light Scattering Detector (ELSD) to monitor the progression of the reaction. Approximately 90% of SHPC [1] was coupled to AT [2] over the course of 48 hours, resulting in production of the synthetic phospholipid product [3] (Figure 1A,B). This relatively slow reaction time is likely due to the dilute reaction conditions, the weak nucleophile catalyst, and the stoichiometric reactant mixture. It should be noted that the progression of the reaction under these disadvantageous reaction conditions to near-completion is another illustration of the capabilities of the thiol-Michael addition reaction.

Certain alkene substituents, for example maleimides, and certain conditions, such as highly polar solvents, have been demonstrated to cause "catalyst-free," solvent-mediated thiol-Michael addition[46,47]. Here, to assess whether a catalyst is necessary for this reaction, SHPC [1] (5mM) and AT [2] (5mM) were mixed in the absence of any catalyst. Over the course of 48 hours, approximately 50% of SHPC was consumed resulting in formation of phospholipid [3]. However, this insufficient degree of conversion demonstrates the need for a catalyst to reach satisfactory conversion under the desired conditions (Figure 1C,D).

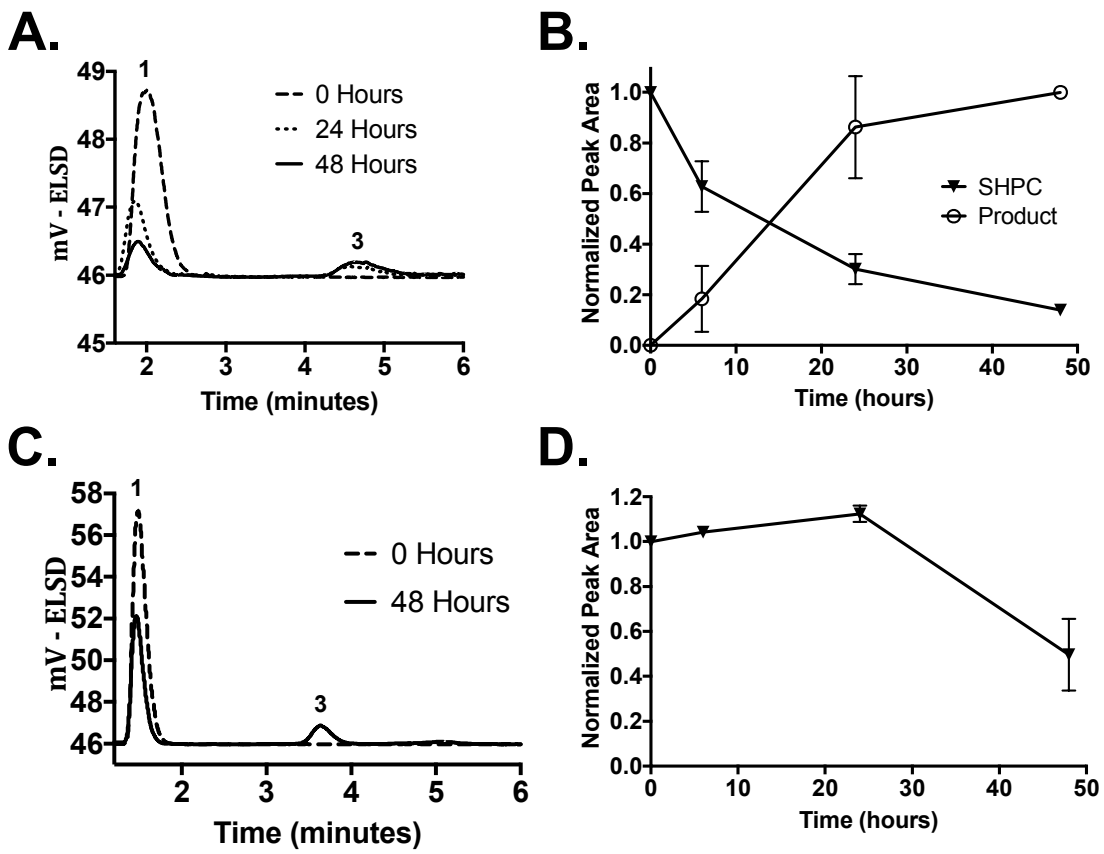

Figure 1. LC-MS coupled with an Evaporative Light Scattering Detector (ELSD) monitoring the progression of the thiol-Michael addition reaction. Reaction solutions of 5mM thiol lysolipid (SHPC) [1], 5mM aliphatic acrylate tail [2], and 2.5mM 2-methylimidazole catalyst were mixed and sampled at various time points to determine conversion (A). SHPC peak area, normalized to 0 hours, and product peak area, normalized to 48 hours, demonstrate almost 90% conversion over the course of 48 hours (B). When catalyst is absent, the reaction occurs to approximately 50% conversion over the course of 48 hours (C,D).

Fluorescence microscopy and cryo-TEM enable imaging of the lipid assemblies. In this way, it is possible to determine the ability of the phospholipid products to self-assemble into lipid vesicles, or liposomes. For fluorescence

microscopy, the AT and reduced SHPC (5mM) were mixed in the presence of 2-methylimidazole catalyst (2.5mM) and a membrane bound, fluorescent dye, rhodamine-DHPE (2uM). Following mixing, a drop was placed on a sealed slide and allowed to develop at room temperature. Fluorescence microscopy verified the presence of liposomal structures following 48 hours of development, as evidenced by a brightly fluorescent membrane surrounding a dark interior (Figure 2A). Cryo-TEM was conducted on the samples to verify the formation of lipid bilayers by thioether-containing phospholipids. Samples were prepared as in the fluorescence microscopy experiments, though excluding rhodamine-DHPE, and subsequently frozen following 48 hours of development. Cryo-TEM images show the presence of lipid bilayer structures in single rings rather than stacked lamellae, indicating that thiol-Michael addition mediated liposome formation using 2.5mM 2-methylimidazole catalyst results in predominantly unilamellar liposomes (Figure 2B). This configuration makes this *in situ* formation method particularly useful for applications requiring unilamellar structures for imaging purposes[48] as it results in vesicular structures over a micron in diameter directly from the reaction mixture and without any requirement of further processing.

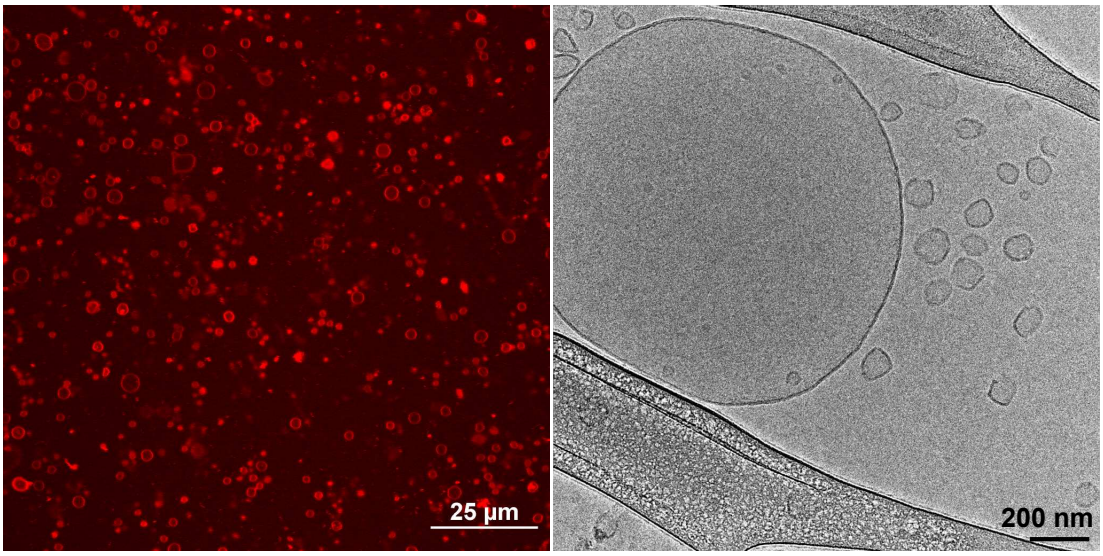

Figure 2. Microscopy images of liposomes assembled from thioether-containing phospholipid products [3]. 5mM reduced SHPC and aliphatic AT were reacted in the presence of 2.5mM 2-methylimidazole. For fluorescence microscopy imaging, 2uM rhodamine-DHPE was included in the reaction mixture. After 48 hours of reaction, fluorescence microscopy demonstrated liposome formation (left) with most liposomes assembled in a unilamellar fashion as demonstrated using cryo-TEM (right).

Modulating the catalyst concentration also enabled control over the lamellarity of the synthetic liposomes formed using the *in situ* formation technique. While 2.5mM 2-methylimidazole catalyst resulted in predominantly unilamellar liposomes, an increase in the catalyst concentration resulted in multilamellar structures. To monitor the reaction with greater catalyst concentrations, LC-MS-ELSD samples were prepared as stated previously ([SHPC]=[AT]=5mm) with 2-methylimidazole at a concentration of 25mM. Samples were taken at various times and injected onto the LC-MS-ELSD. After 48 hours, the reaction reached approximately 90% conversion, similar to the 2.5mM 2-methylimidazole samples.

However, the initial reaction rate was greater with approximately 60% conversion occurring in the first 6 hours while the reactions with 2.5mM 2-methylimidazole only reached approximately 40% conversion over the same period (figure 3A). To assess lamellarity, samples were prepared for fluorescence microscopy imaging ([SHPC]=[AT]=5mM, [2-methylimidazole]=25mM, [rh-DHPE]=1-2μM) and for cryo-TEM ([SHPC]=[AT]=5mM, [2-methylimidazole]=25mM). Fluorescence microscopy verified the assembly of giant (greater than 1 micron in diameter) liposomes (figure 3B) while cryo-TEM enabled imaging of lipid bilayers assembled in concentric rings, thereby verifying multilamellarity (figure 3C). This dependency on catalyst concentration for liposome lamellarity suggests that as lipid bilayers grow from oil droplets stabilized by lysolipids, as observed previously[35], sufficient catalyst concentrations may diffuse across the forming bilayers to initiate new bilayer growth from the droplet surface. This behavior prompts the formation of bilayers within bilayers, or multilamellar structures. Control over liposome lamellarity makes this formation technique useful for not only lipid functionalization but also for producing a range of assembly structures for a wide range of applications.

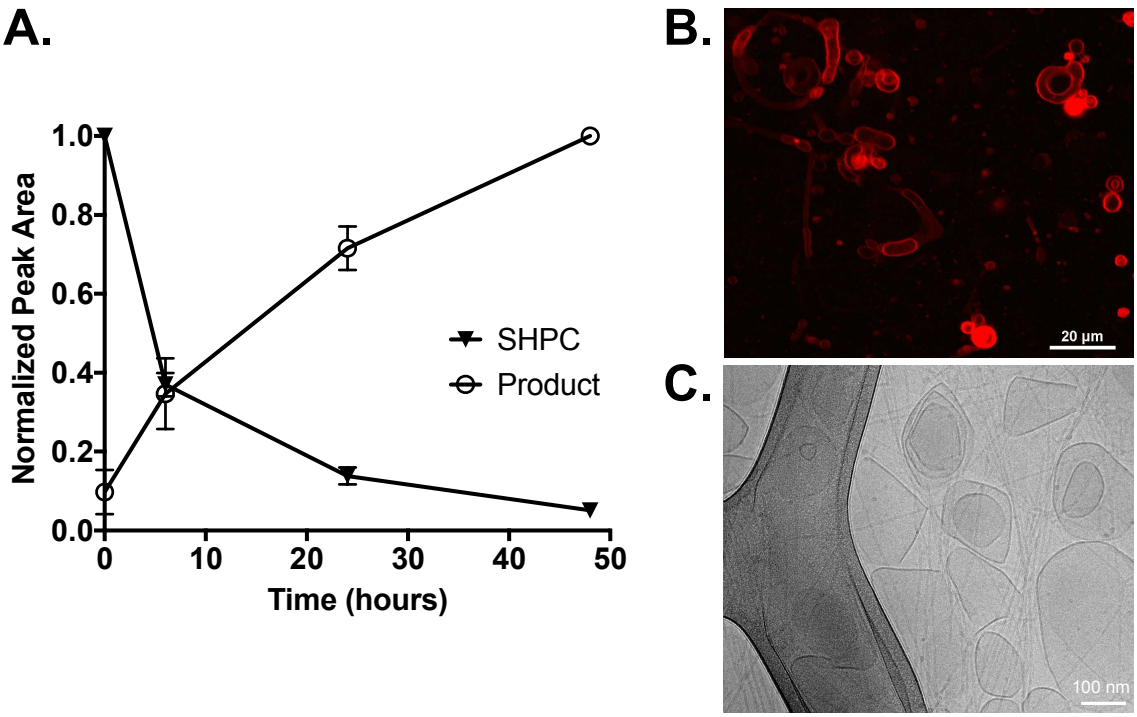

Figure 3. Formation of multilamellar liposomes *via* increased catalyst concentration. Reaction of SHPC and AT (5mM) with increased 2-methylimidazole (25mM) results in approximately 60% conversion over the first 6 hours and 90% over 48 hours (A). Liposomes formed using this increased catalyst concentration result in multilamellar structures as evidenced using fluorescence microscopy (B) and cryo-TEM (C).

Demonstration of the *facile* incorporation of functional moieties into the phospholipid structure

To demonstrate the utility of the thiol-Michael induced formation of phospholipids capable of self-assembling into liposomal structures and to highlight the capacity of this approach to incorporate a variety of acrylic (or other) moieties, a second molecule capable of modifying the characteristics of the liposome system was reacted and incorporated into the phospholipid. A new aliphatic tail was

designed and synthesized with an acrylate functionality for the thiol-Michael coupling as well as a terminal alkyne capable of a number of subsequent reactions. In particular, alkynes are orthogonal to the thiol-Michael addition reaction, providing a downstream functionality for a variety of reactions such as copper-catalyzed azide-alkyne cycloaddition (CUAAC)[49,50], radical-mediated polymerization or radical-mediated thiol-yne addition[51,52]. This reactive capability could be used to modify the vesicle structure or characteristics, such as temporary enhancement of the permeability of the liposome systems upon polymerization as has been demonstrated in the literature[29,30] (scheme 2).

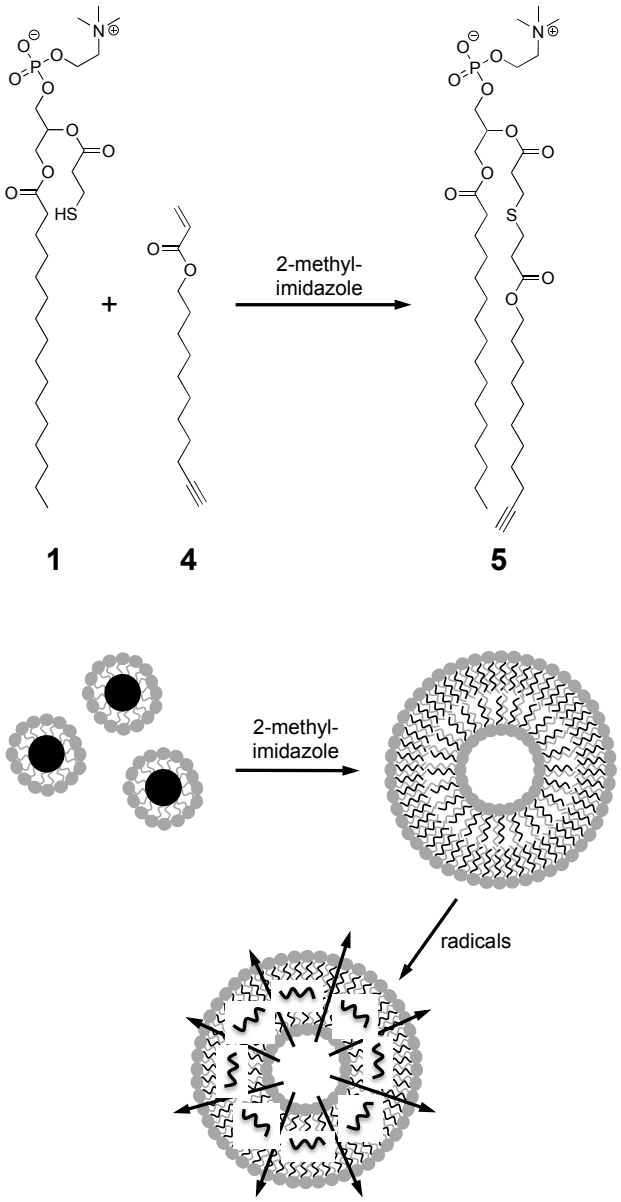

Scheme 2. A schematic illustrating the formation of a designer lipid bearing a terminal alkyne using the thiol-Michael formation method. A new terminal alkyne functionalized AT [4] couples to SHPC [1] in the presence of 2-methylimidazole resulting in liposomes with terminal alkynes buried in their hydrophobic core. These liposomes themselves enable subsequent modification of the membrane characteristics or behavior and as a whole demonstrate the ability to incorporate a wide array of new functionalities using this formation chemistry. As one example of characteristics enabled

with this formulation, homopolymerization could be used to temporarily enhance permeability upon the generation of radicals.

Samples were injected into the LC-MS-ELSD to determine the reaction progress with samples prepared from stoichiometric reactants ([reduced SHPC]=[tail]=5mM and [2-methylimidazole]=2.5mM) including the acrylate-alkyne tail in place of the aliphatic acrylate tail. Additionally, a photoinitiator, lithium phenyl-2,4,6-trimethylbenzoylphosphinate (LAP), was included at a concentration of 5mM to enable subsequent photopolymerization and reaction of the alkyne tail following vesicle formation. Forty-eight hours after mixing, the reaction reached approximately 90% conversion (Figure 4A). The vesicle-containing solution was subsequently irradiated using 400-500nm light at 10mW/cm^2 for 10 minutes to react the alkyne. Injection of the sample on analytical LC-MS-ELSD after irradiation shows complete disappearance of the phospholipid product [5] upon radical generation, due to homopolymerization[52]. Lack of appearance of a new peak in the ELSD chromatogram suggests that the increased hydrophobic character of the polymer results in extensive interaction with the HPLC column causing increased retention, or the size of the polymer product results in removal from the flow by filtration upstream of column separation. Additionally, the disappearance of the phospholipid peak, without equivalent loss of SHPC, promotes the idea that phospholipid product [5] is undergoing homopolymerization and not thiol-yne reactions. To verify the persistence of liposome assembly in the presence of the terminal alkyne functionality, fluorescence microscopy was employed. Mixtures were prepared ([SHPC]=[alkyne AT]=[LAP]=5mM, [2-methylimidazole]=2.5mM,

[rhodamine-DHPE]=2 μM, [fluorescein]=500 μM) and placed in a sealed glass slide. Fluorescence microscopy verified the assembly of giant liposomes following 48 hours of development (figure 4B).

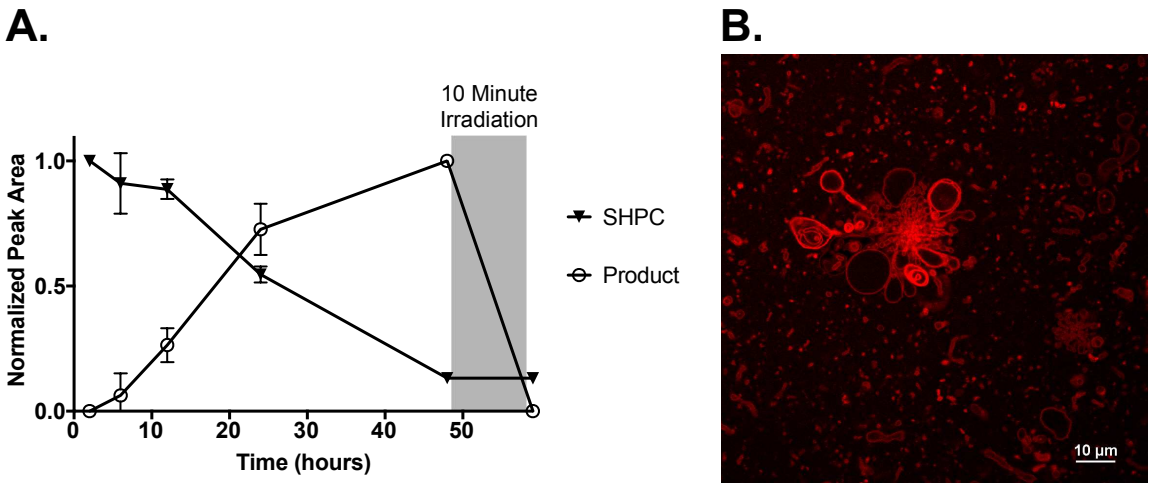

Figure 4. Designer lipid with terminal alkyne functionality synthesized using thiol-Michael addition. LC-MS with ELSD tracks the formation reaction with SHPC peak values normalized to the peak area at 0 hours while product peak values were normalized to the peak area at 48 hours. SHPC [1] and an alkyne-terminated acrylate tail [4] were reacted in the presence of 2.5mM 2-methylimidazole and 5mM LAP photoinitiator resulting in nearly 90% conversion to phospholipid [5] over the course of 48 hours. Subsequently, alkyne-functionalized phospholipids were irradiated with 10mW/cm^2 400-500nm light for 10 minutes, resulting in complete consumption of the phospholipid as the alkyne polymerizes (A). Fluorescence microscopy verified the assembly of functionalized lipids into giant liposomes (B).

These results illustrate the ability to form liposomes *in situ* while incorporating new functionalities into the lipid structure by utilizing the thiol-Michael coupling reaction to functionalize the phospholipid. This formation reaction becomes part of a two-step formation and modification system where

lipids can be functionalized with any of a wide range of compounds bearing electron deficient double bonds in the presence of nucleophilic catalysts followed by a second stimulus to use the incorporated moiety to enact changes in the bilayer characteristics or behavior. An added benefit of the system is the linkage connecting the lysolipid with its primary thiol is part of a class highly sensitive to hydrolytic degradation, offering future opportunities in pH-sensitive lipid degradation or triggered release of attached molecules. It should be noted also that free thiols present in biological materials enable labelling of macromolecules using this chemistry but also require attention as a potential cause of side product formation.

Conclusions

Synthetic liposomal systems have a vast array of potential applications, many of which require enhanced characteristics, tunable responses or modified behavior of the vesicles. The use of thiol-Michael click reactions for forming phospholipids to enable the *facile* incorporation of novel functionalities into the phospholipid structure is demonstrated here through the coupling of acrylate-functional tails with a thiol-functional lysolipid. This approach is compatible with the use of a wide array of acrylate, vinyl sulfone, maleimide and other functionalized compounds available commercially or readily synthesized.

The covalent coupling of thiol-functionalized lysolipids and acrylate functionalized tails using the thiol-Michael reaction enabled generation of synthetic phospholipids, and by extension liposomes, *in situ.* Assembled lipids formed giant vesicles with control over lamellarity making them highly useful for applications

such as membrane dynamics studies and artificial cell membranes. By further modification of the acrylate tail, the ability to readily incorporate new characteristics or behaviors into the final lipid structure was demonstrated. This two-step process added a terminal alkyne tail to SHPC *via* thiol-Michael addition to produce phospholipids capable of assembling into liposomes. After the coupling reaction was complete, polymerization initiated by visible-light induced radical generation resulted in triggered homopolymerization of the lipid tails. This approach is suitable for incorporating functionalities needed to achieve a range of synthetic behaviors or characteristics based upon moieties coupled into the phospholipid structure.

Materials and Methods

General. ^{1}H nuclear magnetic resonance (NMR) spectra for product verification were gathered on a Bruker Ascend 400 spectrometer. Reactions were monitored on an Agilent 1100 Series HPLC fitted with an Agilent Zorbax 5um 4.6x50mm C8 column coupled with Agilent G1946D Mass Spectrometer and SedeX Evaporative Light Scattering Detector.

LAP was synthesized following a previously published method[53] and other compounds were purchased from standard sources and were used as received.

Synthesis of Thiol Lysolipid (SHPC):

To a dry 10mL round-bottomed flask equipped with magnetic stir bar was added 70mg (0.14mmol, 1 equiv.) 1-palmitoyl-2-hydroxy-*sn*-glycero-3-phosphocholine and 3-3.5mL chloroform. Following stirring for 30 minutes under argon the

solution was cooled to 0°C and 60mg (0.28mmol, 2 equiv.) 3,3'-dithiodipropionic acid, 80mg (0.42mmol, 3 equiv.) EDAC and 5mg (0.042mmol, 0.3 equiv.) DMAP was added while stirring. The solution was allowed to react overnight under argon. Following reaction, the $CHCl_3$ was removed and products were dissolved in H_20 for 30 minutes. This solution was transferred to 1,000MW cutoff dialysis tubing and dialyzed overnight. Following dialysis, the solution was transferred to a vial equipped with stir bar and 200mg (0.7mmol, 5 equiv.) TCEP-HCl was added. 1M NaOH was added dropwise to neutralize the solution followed by spinning overnight. This solution was then transferred to fresh 1,000MW cutoff dialysis tubing for overnight dialysis. The product was lyophilized to produce a white powder. Yield = 71% ^{1}H NMR (400mHz, $CDCl_3$) δ: 5.24 (m, 1H), 4.36 (dd, J=12.1, 3.0 Hz, 1H), 4.27 (m, 2H), 4.15 (dd, J=12.1, 7.4 Hz, 1H), 3.95 (m, 2H), 3.75 (m, 2H), 3.32 (s, 9H), 2.74 (m, 2H), 2.67 (m, 2H), 2.28 (m, 2H), 1.80 (t, J=8.2 Hz, 1H), 1.57 (m, 2H), 1.25 (m, 24H), 0.86 (t, 3H). ^{13}C NMR (101 MHz, $CDCl_3$) δ = 173.7, 171.2, 71.3, 66.3, 63.6, 62.9, 59.4, 54.4, 38.6, 34.2, 32.1, 29.8, 29.8, 29.8, 29.8, 29.8, 29.8, 29.7, 29.5, 29.5, 29.3, 25.0, 22.8, 19.8, 14.3. HRMS *m/z*: calcd. for $[C_{27}H_{54}NO_8PS+Cl]^-$ 618.3002; found 618.3032.

Synthesis of Dodecyl Acrylate:

To a round bottom flask with stir bar was added 1.86g (10mmol, 1 equiv.) 1-dodecanol in 10mL THF and allowed to dissolve. 10mL of a THF mixture with 1.02g (10mmol, 1 equiv.) TEA was added to the round bottom and cooled to 0°C. 1.09g (12mmol, 1.2 equiv.) acryloyl chloride was added dropwise and the solution was allowed to equilibrate to room temperature. Stirring continued for at least 3 hours.

Dodecyl acrylate product was extracted with methylene chloride and washed with water. ^{1}H NMR (400mHz, $CDCl_3$) δ: 6.35 (dd, J=17.3, 1.6 Hz, 1H), 6.07 (dd, J=17.3, 10.4 Hz, 1H), 5.75 (dd, J=10.4, 1.6 Hz, 1H), 4.10 (t, J=6.8 Hz, 2H), 1.62 (m, 2H), 1.23 (m, 18H), 0.83 (m, 3H).

Synthesis of Alkyne-Acrylate Tail:

To a round bottom flask with stir bar was added 0.57mL (3 mmol, 1 equiv.) 10-undecyn-1-ol, 1.25mL (9 mmol, 3 equiv.) TEA and 33mg (0.15mmol, 0.05 equiv.) BHT in 15mL methylene chloride under nitrogen. The mixture was cooled to 0^{o}C and 0.36mL (4.5mmol, 1.5 equiv.) acryloyl chloride was added dropwise. 36mg (0.3 mmol, 0.1 equiv.) DMAP was added and the mixture was allowed to equilibrate to room temperature and left to react overnight. The product was washed with sodium bicarbonate, water and brine, dried and filtered before methylene chloride was removed leaving the product as an oil. Yield = 69% ^{1}H NMR (400mHz, $CDCl_3$) δ: 6.40 (dd, J=17.3, 1.5 Hz, 1H), 6.12 (dd, J=17.3, 10.4 Hz, 1H), 5.81 (dd, J=10.4, 1.5 Hz, 1H), 4.14 (t, J=6.7 Hz, 2H), 2.18 (td, J=7.1, 2.6 Hz, 2H), 1.94 (t, J=2.7 Hz, 1H), 1.66 (m, 2H), 1.57-1.44 (m, 2H), 1.42-1.2 (m, 10H)

Preparation of Lipid Solutions. Prior to use, SHPC was reduced overnight in an equimolar mixture of TCEP-HCl and NaOH in a 2:1 SHPC:TCEP solution. For monitoring of the phospholipid coupling reaction *via* LCMS, a 100uL solution was prepared of aliphatic acrylate in water (5mM), reduced SHPC mixture (5mM SHPC), and 2-methylimidazole (2.5mM or 25mM) in HPLC vials fitted with 350uL Supelco glass inserts. The solution was then left at room temperature to react.

Fluorescence microscopy samples were prepared similarly ([reduced SHPC]=[acrylate tail] = 5mM, [2-methylimidazole]= 2.5mM or 25mM) with the addition of 1-2μM rhodamine-DHPE. Samples were mixed, sealed under coverslips, and allowed to develop for 48 hours prior to imaging.

Polymerizeable lipids were prepared similarly to those described above ([reduced SHPC]=[alkyne AT]=5mM, [2-methylimidazole]=2.5mM, and [LAP]=5mM, as well as [rhodamine-DHPE]=2μM and [fluorescein]=500 μM if sample was to be imaged under fluorescence microscopy).

Microscope Imaging. Fluorescence imaging was performed using a Nikon A1R laser scanning confocal microscope equipped with Nikon Elements software version 4.20. In all cases, a 561nm laser was employed to excite the rhodamine-DHPE. For acquisition of TEM images, 4 μl of sample solution was transferred onto a lacey holey-carbon grid, blotted for 1-2 seconds, and then plunge-frozen using an FEI-Vitrobot Mark IV at room temperature. The resulting vitrified sample was imaged on an FEI Tecnai F20 FEG-TEM, operating at 200kV and 25,000x magnification, using a Gatan US4000 CCD camera. The electron dose per image was limited to 20 electrons/$\mathbf{Å^2}$, with a defocus of -2μm, using the low-dose mode of Serial EM acquisition software.

LC-MS of Product Formation. Phospholipid formation was conducted in HPLC vials fitted with 350uL glass inserts as described above with 5uL samples taken over the course of the reaction. Samples were injected onto an analytical Agilent LC-MS

with SedeX Evaporative Light Scattering Detector controlled by ChemStation software and fitted with Agilent Zorbax 5um 4.6x50mm C8 column column. A binary solvent system of 0.1% formic acid in water and methanol was used at a flow rate of 1mL/minute for the 25mM 2-methylimidazole reaction while 0.1% formic acid in 5:4:1 isopropanol:water:methanol and methanol was used at a flow rate of 0.9mL/minute for all other reactions. Peak areas of SHPC precursors were normalized to the peak area measured at 0 hours while products were normalized to the peak area at 48 hours. Degree of conversion was calculated from the consumption of SHPC over the course of the reaction, with the assumption that all SHPC was converted to phospholipid product, an assumption made due to the specificity of the reaction and the lack of any other product peak appearance on the HPLC chromatogram

Acknowledgements. This research was supported by the U.S. Army Research Office through the Multidisciplinary University Research Initiatives (MURI) program [Award No. W911NF-13-1- 0383] and through the National Science Foundation (NSF) – Materials Research Science and Engineering Center (MRSEC) [Grant number: DMR 1420736). The authors would like to thank Joe Dragavon, Jian Tay, and the BioFrontiers Advanced Light Microscopy Core for their microscopy support. Electron microscopy was done at the University of Colorado, Boulder EM Services core facility in MCDB, with the technical assistance of facility staff.

Conflicts of interest

There are no conflicts to declare.

6. References

1 A. Puri, K. Loomis, B. Smith, J.-H. Lee, A. Yavlovich, E. Heldman and R. Blumenthal, *Crit. Rev. Ther. Drug Carrier Syst.*, 2009, **26**, 523–580.
2 A. Yavlovich, B. Smith, K. Gupta, R. Blumenthal and A. Puri, *Mol. Membr. Biol.*, 2010, **27**, 364–381.
3 T. M. Allen and P. R. Cullis, *Adv. Drug Deliv. Rev.*, 2013, **65**, 36–48.
4 P. G. Gregoriadis and A. T. Florence, *Drugs*, 2012, **45**, 15–28.
5 T. M. Allen, *Trends Pharmacol. Sci.*, 1994, **15**, 215–220.
6 A. Lohani and A. Verma, *J. Cosmet. Laser Ther.*, 2017, **19**, 485–493.
7 F. Guo, M. Lin, Y. Gu, X. Zhao and G. Hu, *Eur. Food Res. Technol.*, 2015, **240**, 1013–1021.
8 H. R. A. Ashtiani, P. Bishe, N.-A. Lashgari, M. A. Nilforoushzadeh and S. Zare, *J. Skin Stem Cell*, , DOI:10.5812/jssc.65815.
9 E. Altamura, F. Milano, R. R. Tangorra, M. Trotta, O. H. Omar, P. Stano and F. Mavelli, *Proc. Natl. Acad. Sci.*, 2017, **114**, 3837–3842.
10 B. Ploier and A. K. Menon, *JoVE J. Vis. Exp.*, 2016, e54635–e54635.
11 K. Oglecka, J. Sanborn, A. N. Parikh and R. S. Kraut, *Membr. Physiol. Membr. Biophys.*, 2012, **3**, 120.
12 J. Lorent, C. S. Le Duff, J. Quetin-Leclercq and M.-P. Mingeot-Leclercq, *J. Biol. Chem.*, 2013, **288**, 14000–14017.
13 G. Sessa and G. Weissmann, *J. Lipid Res.*, 1968, **9**, 310–318.
14 B. C. Buddingh' and J. C. M. van Hest, *Acc. Chem. Res.*, 2017, **50**, 769–777.
15 J. C. Blain and J. W. Szostak, *Annu. Rev. Biochem.*, 2014, **83**, 615–640.
16 S. Matosevic, *BioEssays*, 2012, **34**, 992–1001.
17 G. Murtas, *Mol. Biosyst.*, 2009, **5**, 1292–1297.
18 V. Noireaux and A. Libchaber, *Proc. Natl. Acad. Sci. U. S. A.*, 2004, **101**, 17669–17674.
19 Y. Qiao, M. Li, R. Booth and S. Mann, *Nat. Chem.*, 2017, **9**, 110.
20 W. Zong, S. Ma, X. Zhang, X. Wang, Q. Li and X. Han, *J. Am. Chem. Soc.*, 2017, **139**, 9955–9960.
21 K. Kurihara, M. Tamura, K. Shohda, T. Toyota, K. Suzuki and T. Sugawara, *Nat. Chem.*, 2011, **3**, 775–781.
22 S. Kulin, R. Kishore, K. Helmerson and L. Locascio, *Langmuir*, 2003, **19**, 8206–8210.
23 Y. Elani, R. V. Law and O. Ces, *Nat. Commun.*, 2014, **5**, 5305.
24 J. Yu, H. Guan and D. Chi, *J. Solid State Electrochem.*, 2017, **21**, 1175–1183.
25 Y. Barenholz, *Handbook of Nonmedical Applications of Liposomes: Volume III: From Design to Microreactors*, CRC Press, 2018.
26 A. D. Bangham and R. W. Horne, *J. Mol. Biol.*, 1964, **8**, 660-IN10.
27 A. G. Kohli, P. H. Kierstead, V. J. Venditto, C. L. Walsh and F. C. Szoka, *J. Controlled Release*, 2014, **190**, 274–287.
28 A. M. Bayer, S. Alam, S. I. Mattern-Schain and M. D. Best, *Chem. – Eur. J.*, 2014, **20**, 3350–3357.
29 A. Mueller, B. Bondurant and D. F. O'Brien, *Macromolecules*, 2000, **33**, 4799–4804.

30 A. Yavlovich, A. Singh, R. Blumenthal and A. Puri, *Biochim. Biophys. Acta BBA - Biomembr.*, 2011, **1808**, 117–126.
31 R. H. Bisby, C. Mead and C. G. Morgan, *Biochem. Biophys. Res. Commun.*, 2000, **276**, 169–173.
32 K. A. Carter, S. Shao, M. I. Hoopes, D. Luo, B. Ahsan, V. M. Grigoryants, W. Song, H. Huang, G. Zhang, R. K. Pandey, J. Geng, B. A. Pfeifer, C. P. Scholes, J. Ortega, M. Karttunen and J. F. Lovell, *Nat. Commun.*, 2014, **5**, 3546.
33 E. Huynh, J. F. Lovell, R. Fobel and G. Zheng, *Small*, 2014, **10**, 1184–1193.
34 D. Konetski, T. Gong and C. N. Bowman, *Langmuir*, 2016, **32**, 8195–8201.
35 I. Budin and N. K. Devaraj, *J. Am. Chem. Soc.*, 2012, **134**, 751–753.
36 M. D. Hardy, D. Konetski, C. N. Bowman and N. K. Devaraj, *Org. Biomol. Chem.*, 2016, **14**, 5555–5558.
37 D. C. Kennedy, C. S. McKay, M. C. B. Legault, D. C. Danielson, J. A. Blake, A. F. Pegoraro, A. Stolow, Z. Mester and J. P. Pezacki, *J. Am. Chem. Soc.*, 2011, **133**, 17993–18001.
38 E. V. Soares, K. Hebbelinck and H. M. Soares, *Can. J. Microbiol.*, 2003, **49**, 336–343.
39 G. J. Brewer, *Chem. Res. Toxicol.*, 2010, **23**, 319–326.
40 A. Seoane, R. J. Brea, A. Fuertes, K. A. Podolsky and N. K. Devaraj, *J. Am. Chem. Soc.*, 2018, **140**, 8388–8391.
41 R. J. Brea, A. K. Rudd and N. K. Devaraj, *Proc. Natl. Acad. Sci.*, 2016, **113**, 8589–8594.
42 D. Konetski, S. Mavila, C. Wang, B. Worrell and C. N. Bowman, *Chem. Commun.*, 2018, **54**, 8108–8111.
43 D. P. Nair, M. Podgórski, S. Chatani, T. Gong, W. Xi, C. R. Fenoli and C. N. Bowman, *Chem. Mater.*, 2014, **26**, 724–744.
44 S. Chatani, T. Gong, B. A. Earle, M. Podgórski and C. N. Bowman, *ACS Macro Lett.*, 2014, **3**, 315–318.
45 W. Xi, M. Krieger, C. J. Kloxin and C. N. Bowman, *Chem. Commun.*, 2013, **49**, 4504–4506.
46 A. B. Lowe, *Polym. Chem.*, 2010, **1**, 17–36.
47 H. Kakwere and S. Perrier, *J. Am. Chem. Soc.*, 2009, **131**, 1889–1895.
48 P. Walde, K. Cosentino, H. Engel and P. Stano, *ChemBioChem*, 2010, **11**, 848–865.
49 V. V. Rostovtsev, L. G. Green, V. V. Fokin and K. B. Sharpless, *Angew. Chem.*, 2002, **114**, 2708–2711.
50 B. T. Worrell, J. A. Malik and V. V. Fokin, *Science*, 2013, **340**, 457–460.
51 C. E. Hoyle, A. B. Lowe and C. N. Bowman, *Chem. Soc. Rev.*, 2010, **39**, 1355–1387.
52 B. D. Fairbanks, T. F. Scott, C. J. Kloxin, K. S. Anseth and C. N. Bowman, *Macromolecules*, 2009, **42**, 211–217.
53 B. D. Fairbanks, M. P. Schwartz, C. N. Bowman and K. S. Anseth, *Biomaterials*, 2009, **30**, 6702–6707.

TOC Graphic

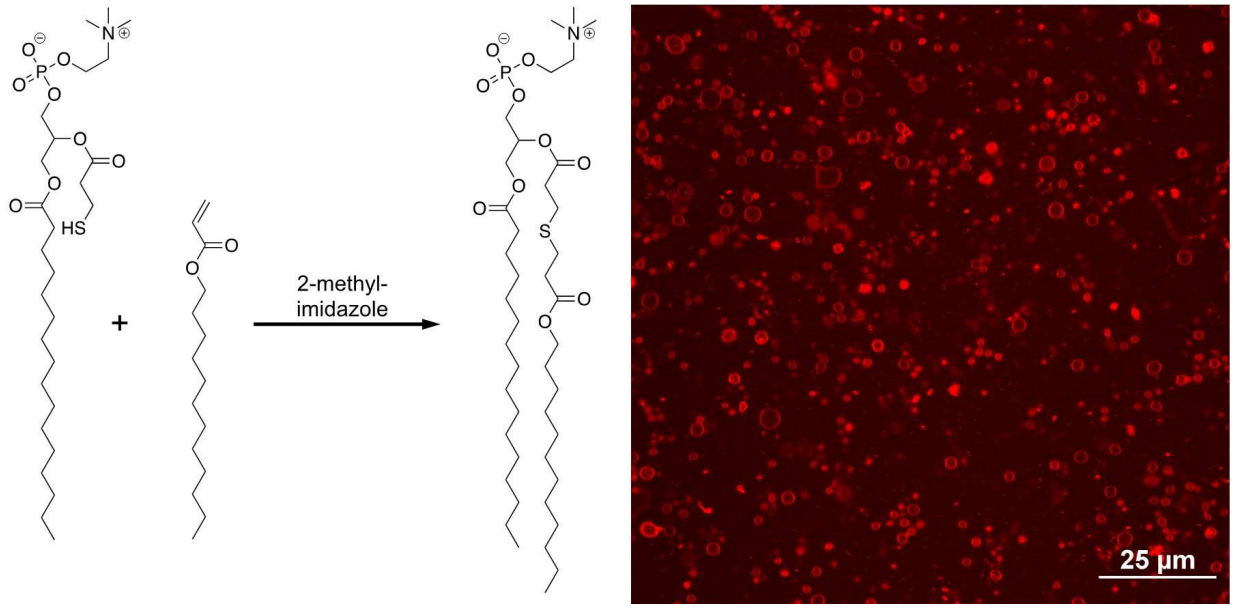

Synthetic liposome formation utilizing the thiol-Michael reaction enables control over liposome lamellarity and facile functionalization of the phospholipid products.